Inorganic Chemistry

Article

pubs.acs.org/IC

Different Rotamer States of Cytosine Nucleobases in Heteronuclear PtPd-, $PtPd_2$, and Pt_2Pd_2Ag Complexes Derived from $[Pt(2,2'\text{-bpy})(1\text{-MeC-}N3)_2]^{2+}$ (1-MeC = 1-Methylcytosine): First Examples of Species with Head–Head Oriented 1-MeC^- Ligands

Lu Yin,[†] Pablo J. Sanz Miguel,*[,‡] Wolf Hiller,[†] and Bernhard Lippert*[,†]

[†]Fakultät Chemie, TU Dortmund, 44221 Dortmund, Germany

[‡]Departamento de Química Inorgánica, Instituto de Síntesis Química y Catálisis Homogénea (ISQCH), Universidad de Zaragoza – CSIC, 50009 Zaragoza, Spain

Supporting Information

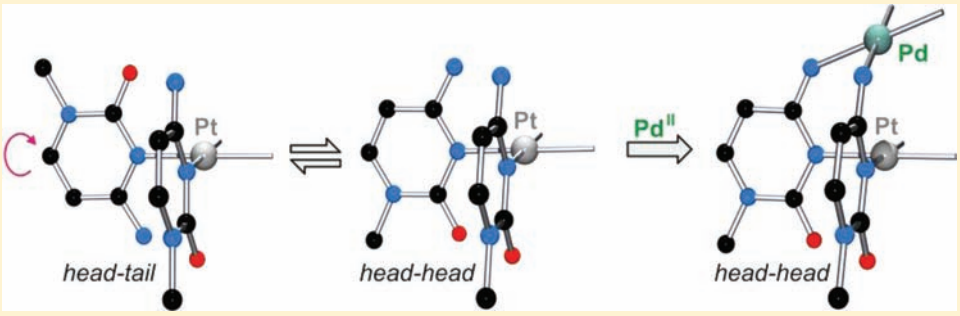

ABSTRACT: $[Pt(2,2'\text{-bpy})(1\text{-MeC-}N3)_2](NO_3)_2$ (**1**) (2,2′-bpy = 2,2′-bipyridine; 1-MeC = 1-methylcytosine) exists in water in an equilibrium of head–tail and head–head rotamers, with the former exceeding the latter by a factor of ca. 20 at room temperature. Nevertheless, **1** reacts with $(en)Pd^{II}$ (en = ethylenediamine) to give preferentially the dinuclear complex $[Pt(2,2'\text{-bpy})(1\text{-MeC}^-\text{-}N3,N4)_2Pd(en)](NO_3)_2\cdot 5H_2O$ (**2**) with head–head arranged 1-methylctosinato (1-MeC^-) ligands and Pd being coordinated to two exocyclic $N4H^-$ positions. Addition of $AgNO_3$ to a solution of **2** leads to formation of a pentanuclear chain compound $[\{Pt(2,2'\text{-bpy})(1\text{-MeC}^-)_2Pd(en)\}_2Ag](NO_3)_5\cdot 14H_2O$ (**5**) in which Ag^+ cross-links two cations of **2** via the four available O2 sites of the 1-MeC^- ligands. **2** and **5** appear to be the first X-ray structurally characterized examples of di- and multinuclear complexes derived from a Pt^{II} species with two cis-positioned cytosinato ligands adopting a head–head arrangement. $(tmeda)Pd^{II}$ (tmeda = *N,N,N′,N′*-tetramethylethylenediamine) and $(2,2'\text{-bpy})Pd^{II}$ behave differently toward **1** in that in their derivatives the head–tail orientation of the 1-MeC^- nucleobases is retained. In $[Pt(2,2'\text{-bpy})(1\text{-MeC}^-)_2\{Pd(2,2'\text{-bpy})\}_2](NO_3)_4\cdot 10H_2O$ (**4**), both $(2,2'\text{-bpy})Pd^{II}$ entities are pairwise bonded to $N4H^-$ and O2 sites of the two 1-MeC^- rings, whereas in $[Pt(2,2'\text{-bpy})(1\text{-MeC}^-)_2\{Pd(tmeda)\}_2(NO_3)](NO_3)_3\cdot 5H_2O$ (**3**) only one of the two $(tmeda)Pd^{II}$ units is chelated to $N4H^-$ and O2. The second $(tmeda)Pd^{II}$ is monofunctionally attached to a single $N4H^-$ site. On the basis of these established binding patterns, ways to the formation of mixed Pt/Pd complexes and possible intermediates are proposed. The methylene protons of the en ligand in **2** are special in that they display two multiplets separated by 0.64 ppm in the ^1H NMR spectrum.

1. INTRODUCTION

Because of their multitopic nature, nucleobases represent versatile ligands for metal ions. Originally examined primarily with the aim of better understanding the basic chemistry underlying metal–nucleic acid interactions in biology,[1,2] relevant studies employing model systems later also dealt with strictly inorganic or physicochemical aspects, which may or may not have any biological relevance. These included, among others, studies of the dynamical behavior of metal–nucleobase complexes,[3] reactivity patterns of coordinated nucleobases (e.g., oxidative[4] or hydrolytic[5] conversions; metal migration processes,[6] condensation reactions[7]), metal–metal interactions in multinuclear complexes,[8] or the generation of supramolecular constructs.[9] Among the nucleobases studied, the pyrimidine base cytosine has been widely applied, and frequently, Pt^{II} and Pt^{IV} complexes were starting points of such work.[10]

Here we describe the behavior of $[Pt(2,2'\text{-bpy})(1\text{-MeC-}N3)_2]^{2+}$ (1-MeC = 1-Methylcytosine) toward $cis\text{-}a_2Pd^{II}$ (a_2 = ethylenediamine, en; *N,N,N′,N′*-tetramethylethylenediamine, tmeda; 2,2′-bipyridine, 2,2′-bpy), which originated from an earlier observation, according to which a heteronuclear $PtPd_2$ complex is formed during the reaction of $cis\text{-}[Pt(NH_3)_2(1\text{-MeC-}N3)_2]^{2+}$ with $(en)Pd^{II}$.[11] In this complex, the two nucleobases adopt a head–tail orientation, with the two

Received: March 7, 2012
Published: June 4, 2012

   dx.doi.org/10.1021/ic3005097 | *Inorg. Chem.* 2012, 51, 6784–6793

(en)Pd^{II} entities bonded to pairs of O2 and deprotonated N4H sites. It has been the explicit goal of our work since quite some time to synthesize cationic multinuclear metal compounds containing two 1-MeC ligands cis to each other and in a head–head arrangement. Our interest in such metal complexes has two routes, namely, to study possible metal–metal interactions in such complexes in analogy to those present in structurally related 1-methyluracilato and 1-methylthyminato complexes of *cis*-a_2Pt^{II} [12] and to probe their potential for noncovalent interactions with double-stranded DNA.[13] As will be demonstrated hereafter, the choice of 2,2′-bpy as the diamine (a_2) ligand in *cis*-$[Pt(a)_2(1\text{-MeC-}N3)_2]^{2+}$ proved fortunate in getting access to such compounds.[14] However, at the same time, it became evident that the choice of the coligand of the Pd entity, hence, en, tmeda, or 2,2′-bpy, was equally important because only with (en)Pd^{II} could the dinuclear head–head complex be isolated in good yield.

2. EXPERIMENTAL SECTION

Preparations. 1-MeC,[15] Pd(2,2′-bpy)Cl_2,[16] Pd(en)Cl_2,[17] Pd(tmeda)Cl_2,[18] and $[Pt(2,2'\text{-bpy})(1\text{-MeC-}N3)_2]^{2+}$ (**1**)[19] were prepared as reported.

Preparation of hh-[Pt(2,2′-bpy)(1-MeC⁻-*N3,N4*)$_2$Pd(en)]-$(NO_3)_2$·5H_2O (2). An aqueous suspension (20 mL) of Pd(en)Cl_2 (950 mg, 4 mmol) and $AgNO_3$ (1.36 g, 8 mmol) was stirred for 12 h at room temperature with daylight excluded. The resultant AgCl precipitate was filtered off, and **1** (726 mg, 1 mmol) was added to the clear filtrate. The pH of the solution (2.3) was brought to 5.2 by means of NaOH, and this solution was stirred at 40 °C for 3 days. The resulting solution was concentrated to a volume of 5 mL at 40 °C on a rotary evaporator. Ten days later, yellow crystals of **2** were collected from the solution and characterized by X-ray crystallography. The isolated yield was 108 mg (11.5%), but according to ^{1}H NMR spectroscopy, **2** is formed in higher yield, ca. 45%. Anal. Calcd. for 3-hydrate of **2**, $C_{22}H_{34}N_{12}O_{11}PdPt$: C, 27.99; H, 3.63; N, 17.80. Found: C, 28.4; H, 3.5; N, 17.8. X-ray crystallography showed the compound to contain five H_2O molecules.

Preparation of [{Pt(2,2′-bpy)(1-MeC⁻)$_2$}{Pd(tmeda)}$_2$(NO$_3$)]-$(NO_3)_3$·5H_2O (3). $AgNO_3$ (1.36 g, 8 mmol) was added to a suspension of Pd(tmeda)Cl_2 (1.76 g, 4 mmol) in 50 mL of water. The mixture was stirred at 40 °C in the dark for 24 h. After filtration of AgCl, complex **1** (726 mg, 1 mmol) was added to the clear filtrate. The pH of the solution was adjusted to 5.2 by adding NaOH (0.1 M) solution. The mixture was stirred at 40 °C for 12 days. The resulting solution was concentrated to a volume of 5 mL at 40 °C on a rotary evaporator. Orange crystals were obtained after 3 days and characterized by X-ray crystallography. The isolated yield was 127 mg (9.2%). Anal. Calcd. for 5-hydrate of **3**, $C_{32}H_{62}N_{16}O_{19}Pd_2Pt$: C, 27.79; H, 4.52; N,16.21. Found: C, 27.8; H, 4.6; N, 16.3.

Preparation of [Pt(2,2′-bpy)(1-MeC⁻)$_2${Pd(2,2′-bpy)}$_2$]-$(NO_3)_4$·10.75H_2O (4). An aqueous suspension (50 mL) of Pd(bpy)Cl_2 (1.34 g, 4 mmol) and $AgNO_3$ (1.36 g, 8 mmol) was stirred for 12 h at 40 °C with daylight excluded and then filtered from AgCl. **1** (726 mg, 1 mmol) was added to the filtrate and stirred at 40 °C for 12 h. The solution was concentrated to 5 mL. After 5 days, red crystals were obtained by slow evaporation of the solution at 4 °C and characterized by X-ray crystallography. The yield was 136 mg (8.7%). Anal. Calcd. for 4.75 hydrated **4**, $C_{40}H_{57.5}N_{16}O_{24.75}Pd_2Pt$: C, 32.94; H, 3.14; N, 15.36. Found: C, 33.2; H, 3.1; N, 15.4. X-ray crystallography showed the compound to contain 10.75 H_2O molecules.

Preparation of [{Pt(2,2′-bpy)(1-MeC⁻)$_2$Pd(en)}$_2$Ag]-$(NO_3)_5$·14H_2O (5). A solution of **2** (951 mg, 1 mmol) and $AgNO_3$ (340 mg, 2 mmol) in 5 mL of H_2O was stirred at room temperature for 1 h. After 7 days, pale yellow crystals were obtained by slow evaporation of the solution at 4 °C and characterized by X-ray crystallography. The yield was 265 mg (24.1%). Anal. Calcd. for **5**, $C_{44}H_{84}AgN_{25}O_{33}Pd_2Pt_2$: C, 24.00; H, 3.84; N, 15.90. Found: C, 23.9; H, 3.9; N, 15.9.

Instrumentation. One- and two-dimensional ^{1}H NMR spectra were recorded on Varian Mercury 200 FT NMR, Bruker DRX 300, Bruker DRX 400, Bruker DRX 500, and Varian Unity/NOVA-500 instruments. TSP (δ = 0 ppm for $Si(CH_3)_3$ signal) was used as an internal reference in D_2O. 64 kb data points were recorded for the ^{1}H NMR spectra using 30° pulses and a relaxation delay of 5 s. The residual HDO line was suppressed by transmitter presaturation. The 2D data were performed with the Unity/NOVA-500 with a 5 mm triple resonance probe H(C,X). In this case, 2 kb data and 512 increments were acquired. Heteronuclear single quantum coherence (HSQC), heteronuclear multiple-bond correlation (HMBC), and nuclear Overhauser effect spectrometry (NOESY) were measured in phase sensitive mode. Reported pD values of NMR samples were measured by use of a glass electrode on a pH meter[20] and were obtained by adding 0.4 units to the meter reading. Elemental (C, H, N) analysis data were determined on a Leco CHNS-932 instrument.

X-ray Data Collection. Crystal data, data collection, and refinement parameters for compounds **2**, **3**, **4**, and **5** were recorded on an Oxford Diffraction Xcalibur S diffractometer with graphite monochromated Mo Kα radiation (0.71073 Å). Data reduction was done with CrysAlisPro.[21] All structures were solved by direct methods and refined by full-matrix least-squares methods based on F^2 using SHELXL-97 and WinGX.[22] All nonhydrogen atoms were refined anisotropically, except disordered nitrate atoms in **5**. Several thermal and distance restraints were used to fit some nitrate anions and water molecules of crystallization. All hydrogen atoms were positioned geometrically and refined with isotropic displacement parameters according to the riding model. Calculations were performed with the SHELXL-97 program.[22]

Crystal data for hh-[Pt(2,2′-bpy)(1-MeC⁻-*N3,N4*)$_2$Pd(en)]-$(NO_3)_2$·5H_2O (**2**): $[C_{22}H_{38}N_{12}O_{13}PdPt]$, M = 980.13 g mol^{-1}, yellow prisms, triclinic, space group $P\bar{1}$, a = 11.0364(4) Å, b = 11.6005(7) Å, c = 14.2911(7) Å, α = 79.285(4)°, β = 85.476(4)°, γ = 72.036(4)°, V = 1709.66(15) Å^3, Z = 2, D_{calcd} = 1.904 g cm^{-3}, T = 150(2) K, μ = 4.690 mm^{-1}, 14139 reflections collected, 7747 unique (R_{int} = 0.0383), R_1 [$I > 2\sigma(I)$] = 0.0496, wR_2 (F, all data) = 0.1223, GoF = 0.975. CCDC 870391.

Crystal data for [{Pt(2,2′-bpy)(1-MeC⁻)$_2$}{Pd(tmeda)}$_2$(NO$_3$)]-$(NO_3)_3$·5H_2O (**3**): $[C_{32}H_{62}N_{16}O_{19}Pd_2Pt]$, M = 1382.87 g mol^{-1}, yellow blocks, monoclinic, space group $P2_1/c$, a = 11.3962(5) Å, b = 28.1525(11) Å, c = 15.8563(7) Å, β = 99.897(4)°, V = 5011.5(4) Å^3, Z = 4, D_{calcd} = 1.833 g cm^{-3}, T = 150(2) K, μ = 3.580 mm^{-1}, 23267 reflections collected, 11296 unique (R_{int} = 0.0799), R_1 [$I > 2\sigma(I)$] = 0.0553, wR_2 (F, all data) = 0.1195, GoF = 0.973. CCDC 870392.

Crystal data for [Pt(2,2′-bpy)(1-MeC⁻)$_2${Pd(2,2′-bpy)}$_2$]-$(NO_3)_4$·10.75H_2O (**4**): $[C_{160}H_{230}N_{64}O_{99}Pd_8Pt_4]$, M = 6265.64 g mol^{-1}, red blocks, monoclinic, space group $P2_1/c$, a = 25.3342(9) Å, b = 19.9881(4) Å, c = 26.8973(17) Å, β = 120.747(3)°, V = 11705.7(9) Å^3, Z = 2, D_{calcd} = 1.778 g cm^{-3}, T = 150(2) K, μ = 3.085 mm^{-1}, 134046 reflections collected, 28861 unique (R_{int} = 0.0732), R_1 [$I > 2\sigma(I)$] = 0.0837, wR_2 (F, all data) = 0.2767, GoF = 1.003. CCDC 870393.

Crystal data for [{Pt(2,2′-bpy)(1-MeC⁻)$_2$Pd(en)}$_2$Ag]-$(NO_3)_5$·14H_2O (**5**): $[C_{44}H_{84}AgN_{25}O_{33}Pd_2Pt_2]$, M = 2202.21 g mol^{-1}, pale yellow plates, monoclinic, space group $P2_1/c$, a = 16.2123(7) Å, b = 16.7257(6) Å, c = 27.3096(13) Å, β = 98.122(4)°, V = 7331.0(5) Å^3, Z = 4, D_{calcd} = 1.995 g cm^{-3}, T = 150(2) K, μ = 4.649 mm^{-1}, 34578 reflections collected, 16419 unique (R_{int} = 0.0516), R_1 [$I > 2\sigma(I)$] = 0.0542, wR_2 (F, all data) = 0.1399, GoF = 0.998. CCDC 870394.

3. RESULTS AND DISCUSSION

$[Pt(2,2'\text{-bpy})(1\text{-MeC-}N3)_2]^{2+}$ (1). The X-ray crystal structure analysis of the nitrate salt has previously been reported by us.[19] It revealed a head–tail orientation of the two 1-MeC ligands in the solid state. Coordination to Pt takes place via the N3 positions of the model nucleobase. This arrangement is facilitated by two intramolecular hydrogen bonds between pairs of exocyclic $N4H_2$ and C2O groups (2.869, 2.938, 2.966, and

dx.doi.org/10.1021/ic3005097 | Inorg. Chem. 2012, 51, 6784–6793

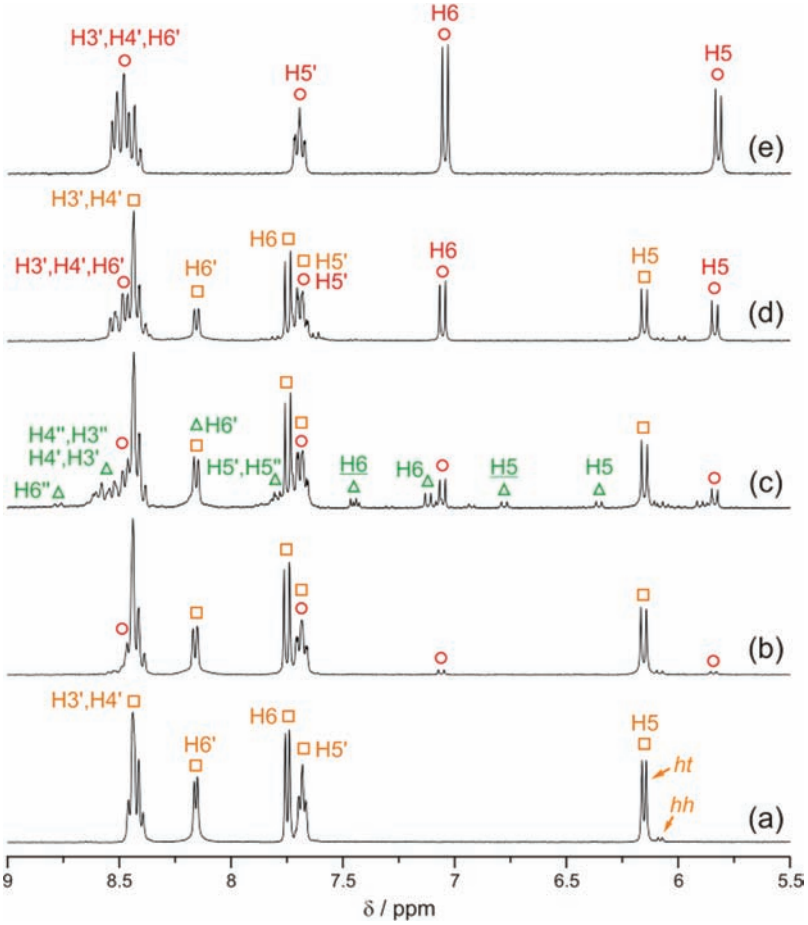

Figure 1. Lowfield portions of ^{1}H NMR spectra (D_2O, pD ≃ 5.2, 22 °C) of (a) starting compound **1**, mixture of **1** and $[Pd(en)(D_2O)_2]^{2+}$ (1:1) after different times (b–d), and the isolated major product **2** (e). Spectra (b–d) were recorded 1, 2, and 11 d after sample preparation. Spectra (b–e) were obtained at 300 MHz, spectrum (a) at 400 MHz. Color codes: orange (**1**), red (**2**), and green (analogue of **3**). Primed numbers refer to 2,2′-bpy resonances.

3.035 Å). The ^{1}H NMR spectrum of **1** in D_2O shows the existence of a major and a minor species. As the dominant species is seen immediately (5 min) after sample preparation, it is assigned to the head–tail rotamer present in the solid state. Only the H5 and CH_3 resonances of the minor species can be observed, whereas H6 is superimposed by the major H6 signal. No individual 2,2′-bpy resonances are detected for the minor species. Resonances of the minor species are seen immediately after dissolving **1** in D_2O, at an intensity of ca. 3% of the major one, but after 30 min and 2 h, relative intensities have grown to 4% and 5%, respectively. Afterward, this ratio does not change (Supporting Information). The minor species is assigned to the head–head rotamer of **1**. Deliberate addition of free 1-MeC clearly rules out that the minor signals are due to an impurity of 1-MeC,[23] and likewise, the presence of a 1:1 complex can be disregarded. Our findings demonstrate that in water the head–tail rotamer of **1** is favored over the head–head rotamer by a factor of ca. 20 but, at the same time, that rotation of the 1-MeC ligands about the Pt–N3 bonds is relatively fast.

Reactions of 1 with (Diamine)Pd^{II}. Figure 1 provides a stack plot of the lowfield portions of ^{1}H NMR spectra (D_2O, pD ≃ 5.2) obtained by reactions of **1** with $[Pd(en)(D_2O)_2]^{2+}$ in a 1:1 ratio. Included are also spectra of **1** in the absence of (en)Pd^{II} and of the isolated major complex **2** formed under these conditions. Product **2** forms in a smooth reaction. Other products occur, in part, only transiently or form and subsequently convert into **2**. X-ray crystallography reveals **2** to be the head–head PtPd species hh-$[Pt(2,2'\text{-bpy})(1\text{-MeC}^-\text{-}N3,N4)_2Pd(en)](NO_3)_2\cdot 5H_2O$ (see below). This feature suggests that this species is a thermodynamically favored one, hence that the head–tail starting compound **1** undergoes nucleobase rotation prior to formation of **2**. We note that in the presence of an excess of (en)Pd^{II} other products are rapidly formed initially but that after longer reaction times again **2** is the preferred species in solution. Figure 2 gives ^{1}H NMR spectra of reaction mixtures of **1** with a 4-fold excess of $[Pd(en)(D_2O)_2]^{2+}$ after various reaction times. Two of the (intermediate) products are marked, which will be discussed later.

Analogous reactions have been carried out also with $[Pd(tmeda)(D_2O)_2]^{2+}$ and with $[Pd(2,2'\text{-bpy})(D_2O)_2]^{2+}$. Given the large number of resonances seen with (en)Pd^{II} (ca. 10–11 sets of cytosine-H5 doublets, at least 10 CH_3 singlets, see Figure 2), we developed a possible reactions scheme (Figure 3), which is based on an educated guess of what might happen in solution, given the existence of four isolated and structurally characterized complexes. The scheme does not differentiate between diamine being en, tmeda, or 2,2′-bpy, even though we note that at least (2,2′-bpy)Pd^{II} behaves differently from (en)Pd^{II} and (tmeda)Pd^{II} (see below), and despite the fact that steric requirements of the diamines likewise may have an influence as to which of the feasible products are formed. As

dx.doi.org/10.1021/ic3005097 | Inorg. Chem. 2012, 51, 6784–6793

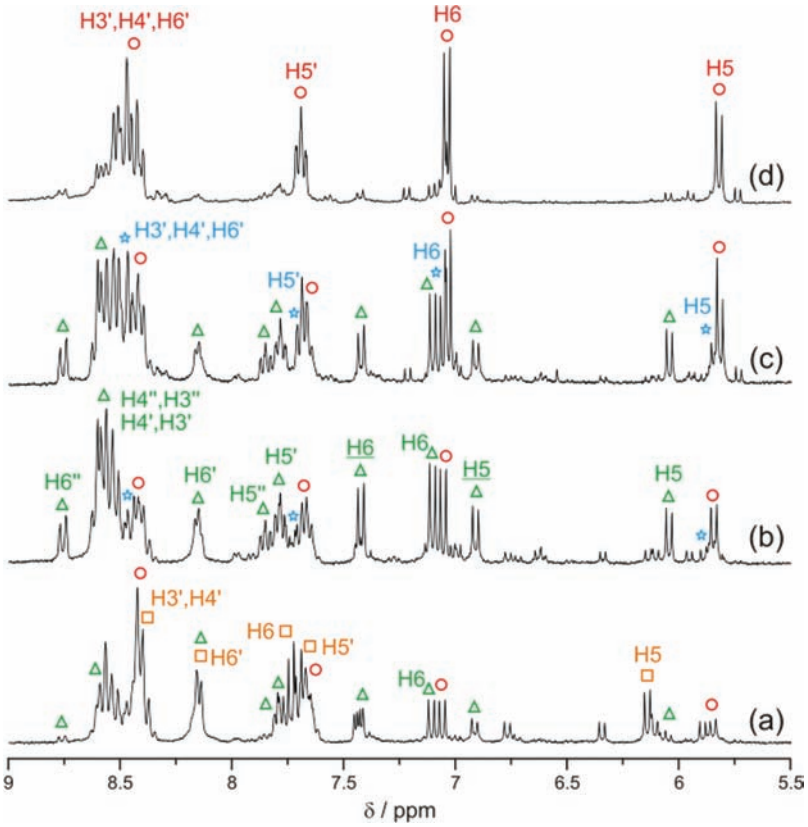

Figure 2. Lowfield portions of ^{1}H NMR spectra (D_2O, pD ≃ 5, 22 °C) of mixture of **1** with an excess of $[Pd(en)(D_2O)_2]^{2+}$ (1:4) after different times: (a) after 30 min, (b) after 2 h, (c) after 4 d, and (d) after 20 d. All spectra were recorded at 300 MHz. Color codes are as in Figure 1. Blue resonances are tentatively assigned to analogue of **4**, hence to symmetrical head−tail PdPtPd species.

outlined below, we propose that Pd coordination to O2 is kinetically favored, but the situation is not as clear-cut as might be expected (c.f. complex 3), and O2 binding, at least in combination with N4 binding, appears to be thermodynamically favorable. In any case, the complicated NMR spectra strongly suggest that not only the thermodynamically most stable products are formed. In that case the number of resonances should be relatively small.

hh-[Pt(2,2′-bpy)(1-MeC$^-$-*N3,N4*)$_2$Pd(en)](NO$_3$)$_2$·5H$_2$O (2). A view of the dinuclear cation of **2** is provided in Figure 4. It represents the first example of a dinuclear Pt^{II}/Pd^{II} complex with head−head oriented 1-methylcytosinato ligands and overall cis-geometries at the two metal ions. Head−tail dinuclear complexes of 1-MeC$^-$ with *cis*-a$_2$Pt^{II} (a= NH$_3$,[24] a$_2$ = en[10b]) and (en)Pd^{II}[25] have been reported before, but these are usually derived from 1:1 complexes upon dimerization. Head−head dinuclear Pt^{II}/Pd^{II} or mixed Pt^{II}/Pd^{II} complexes are common with bridging 1-methyluracilate[12,26] or 1-methylthyminate[27] ligands, and interestingly, these are formed, as in the present case, from the 1:2 complexes, which in the solid state have their two nucleobases in a head−tail arrangement.[28] In dinuclear complexes derived from *trans*-$[Pt(a)_2(1\text{-MeC-}N3)_2]^{2+}$ (a = NH$_3$ or MeNH$_2$), the two bases adopt head−head orientations,[29] again in contrast to the situation of the Pt starting compound in the solid state.[3e]

In **2**, the (2,2′-bpy)Pt^{II} moiety is bonded to N3 sites of 1-MeC$^-$ ligands, and (en)Pd^{II} is bonded to two N4 positions, which have undergone a single deprotonation each. Both possible enantiomers of cation **2** are present in the unit cell, displaying each opposite λ and δ puckers of the en groups. Dihedral angles between metal coordination planes (Pt1N$_4$ and Pd1N$_4$) and the nucleobase rings are Pt1N$_4$/1-MeC$_{(A)}$, 86.4(2)°; Pt1N$_4$/1-MeC$_{(B)}$, 72.0(2)°; Pd1N$_4$/1-MeC$_{(A)}$, 69.1(2)°; Pd1N$_4$/1-MeC$_{(B)}$, 86.7(2)°. As expected, Pt1 is located reasonably close to the cytosine planes to assume essentially sp^2 hybridization of the N3 atoms of both 1-MeC$^-$ ligands: Pt1−1-MeC$_{(A)}$, 0.111(11) Å and Pt1−1-MeC$_{(B)}$, 0.129(11) Å. In contrast, the Pd ion is substantially out of the two cytosinato planes: Pd1−1-MeC$_{(A)}$, 0.545(13) Å and Pd1−1-MeC$_{(B)}$, 0.463(15) Å. However, it is more difficult to relate these figures to the hybridization state of N4, especially since C4−N4 distances do not correspond to true double bonds. In fact, C4−N4 1.250(11) Å for C4b−N4b corresponds to 4.3 σ. These values suggest a considerable degree of softness of the C4−N4 bond upon metal coordination to N4. The metal coordination planes are at a tilt angle of 27.8(2)°, and the cation displays a torsion angle of an average of 14.7°. The distance between both metal centers (Pt1−Pd1, 2.8949(7) Å) is in the range of analogous head−head complexes displaying $\pi-\pi$ stacking interactions between metal (chelating) ligands as, for example, in the case of hh-$[\{Pd(2,2'\text{-bpy})\}_2(1\text{-MeU}^-\text{-}O3,O4)_2]^{2+}$,[26b] where the Pd−Pd separation is 2.848(1) Å. Intermetallic distances relating hh complexes without interaction between coligands are longer: 2.92 − 3.01 Å.

The packing of **2** is dominated by $\pi-\pi$ stacking and hydrogen bonding (Supporting Information). The cations of **2** are arranged in pairs, with 2,2′-bpy ligands of neighboring entities at a stacking distance of 3.3 Å. This motif is repeated along the *a* axis, together with surrounding hydrogen bonding, which involves additional interactions of cations with nitrate

dx.doi.org/10.1021/ic3005097 | Inorg. Chem. 2012, 51, 6784−6793

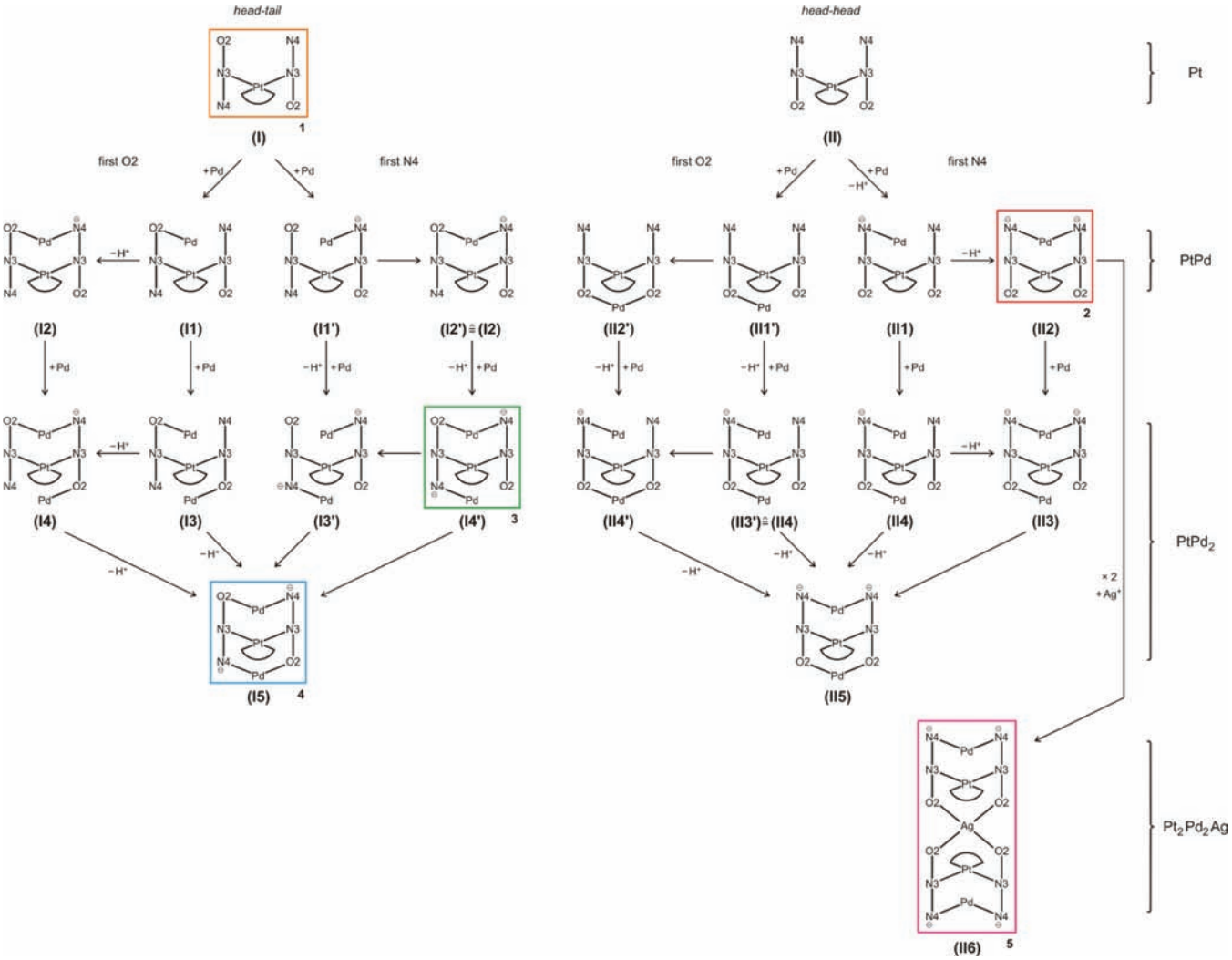

Figure 3. Feasible products formed during the reaction of head−tail and head−head rotamers of $[Pt(2,2'\text{-bpy})(1\text{-MeC-}N3)_2]^{2+}$ (**1**) with *cis*-$[Pd(a)_2(D_2O)_2]^{2+}$. No differentiation between a_2 = en, tmeda, and 2,2′-bpy is made. Boxed-in compounds have been characterized by X-ray analysis. Color codes are as used in Figures 1 and 2. Note that protonation states of exocyclic amino groups are N4 and $N4^-$ for NH_2 and NH^-, respectively.

and water molecules. The packing pattern of **2** is thus markedly different from those found in dinuclear Pt complexes with head−head arranged bridging 1-methyluracilato and 1-methylthyminato ligands.[27] In particular, no formation of intermolecular hydrogen bonds between NH functionalities at the Pt and O acceptors at the nucleobases are observed, which in the case of 1-methyluracilate head−head dimers of *cis*-a_2Pt^{II} can be considered a pattern also seen in partially oxidized "platinum blues".[30]

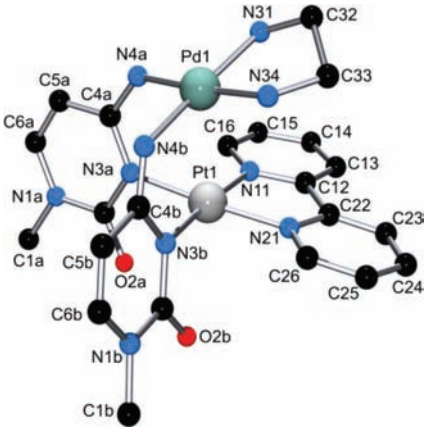

Figure 4. View of molecular cation of **2** with head−head arrangement of 1-MeC^- ligands.

The ^{1}H NMR spectrum of **2** reveals an interesting detail regarding the methylene resonances of the en chelate ring. Unlike in mononuclear (en)M^{II} complexes (M = Pt, Pd), which contain two identical ligands and display a broad, unresolved singlet for the methylene protons, in the spectrum of **2**, these resonances are split into two multiplets of a 1:1 ratio which are separated by 0.64 ppm (Figure 5a and Supporting Information). As confirmed by spin simulation, the methylene protons of the en ligand represent an AA′XX′ spin system with chemical shifts of 2.442 ppm (A, A′) and 1.796 ppm (X, X′) and the following coupling constants (Hz): J(A,X) = −12.82; J(A, X′) = 7.37; J(X′,X′) = 4.05; J(A,A′) = 4.57. Thus, the two protons of each CH_2 are not identical, unlike the carbon atoms as verified in the HSQC spectrum (Supporting Information). The NOESY (Figure 5b) confirms the spatial proximity of the X and X′ protons with the bpy ring protons by giving cross-peaks with the latter. As expected, the CH_2 multiplet at higher field corresponds to X and X′ protons. A complete assignment of

dx.doi.org/10.1021/ic3005097 | *Inorg. Chem.* 2012, 51, 6784−6793

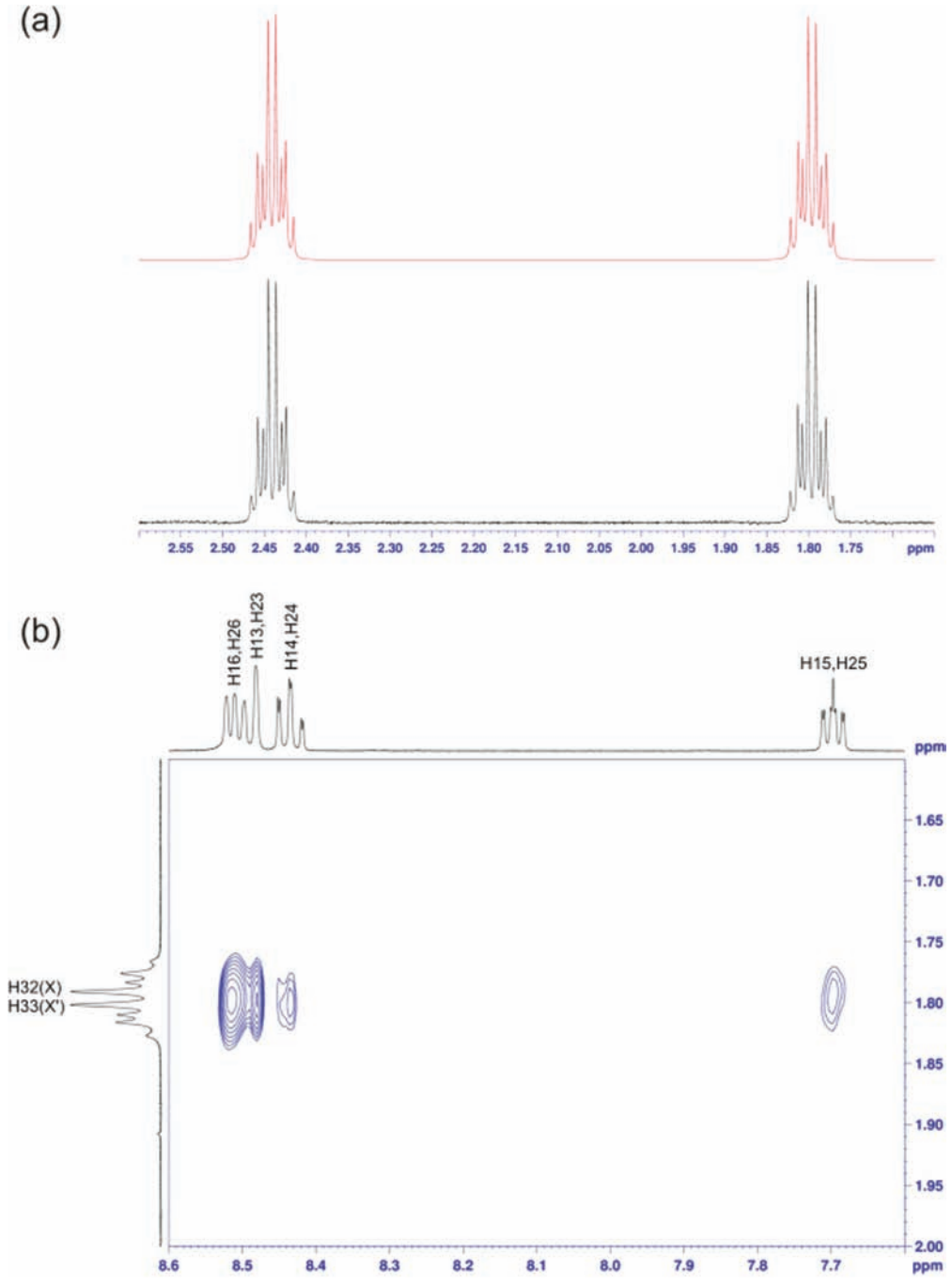

Figure 5. (a) Two methylene multiplets of en ligand in ^{1}H NMR spectrum (D_2O, pD 6.9) of **2** with simulated spectrum on top. (b) Section of NOESY spectrum of **2** displaying the cross-peaks between X, X′, and the bpy protons.

proton and carbon resonances of cation **2** was accomplished by HSQC and HMBC spectra (Supporting Information).

Maintaining the ht-Orientation of 1-MeC$^-$ Ligands. With (tmeda)Pd^{II}, a trinuclear complex [{Pt(2,2′-bpy)(1-MeC$^-$)$_2$}{Pd(tmeda)}$_2$(NO$_3$)](NO$_3$)$_3$·5H$_2$O (**3**) could be isolated and characterized by X-ray crystallography. The cation is shown in Figure 6. As can be seen, the two 1-methylcytosinato ligands are in a head−tail arrangement, but they are nonequivalent, as there is O2, N4H chelation of (tmeda)Pd^{II} on one side (Pd1), yet monodentate binding to N4H only on the other side (Pd2). Pd2 completes its coordination sphere with a nitrate anion. Metal−metal distances within cation **3** are large (Pt1−Pd1, 3.1109(7) Å; Pt1−Pd2, 4.9749(7) Å) as a consequence of steric crowding (tmeda ligands at Pd1) and the orientation of the Pd2 entity, respectively. The palladium atoms are situated out of the planes defined by the cytosine rings. The distance of the nonchelating Pd2 is significantly longer: Pd1−1MeC$_{(A)}$, 0.467(14) Å, vs Pd2−1MeC$_{(B)}$, 0.592(14) Å. The structure itself does not tell whether **3** is a precursor on the way to the symmetrical head−tail PtPdPt species (I5 in Figure 3) or whether it is a derivative of I5 in which the Pd−O2 bond has opened. A view of the packing pattern of **3** in the crystal and selected intermolecular contacts are provided in the Supporting Information.

The ^{1}H NMR spectrum of **3** immediately after dissolving in D_2O is consistent with the presence of two nonequivalent 1-

dx.doi.org/10.1021/ic3005097 | Inorg. Chem. 2012, 51, 6784−6793

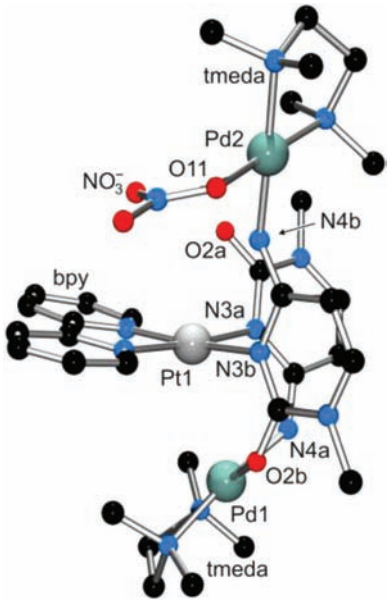

Figure 6. View of cation **3** with atom numbering scheme.

MeC$^-$ rings and with the two halves of 2,2′-bpy being likewise different. Thus, 1-MeC$^-$ resonances (CH_3: 3.39 and 3.48 ppm; H5: 5.89 and 7.09 ppm; H6: 7.11 and 7.37 ppm) are doubled (Supporting Information). New resonances grow in, at the expense of those of **3**. After 1 day, the 500 MHz NMR spectrum reveals ten methyl resonances of 1-MeC/1-MeC$^-$ (3.30−3.61 ppm) and five H5 doublets between 5.80 and 6.40 ppm. A 2D COSY experiment (Supporting Information) permits a partial correlation of cytosine H5 and H6 resonances. After 15 days at room temperature, one species dominates (ca. 50% of total intensities, which has its cytosine resonances at 3.29 (CH_3), 5.87 (H5), and 7.07 ppm (H6). This very same compound, contaminated with some starting compound **1**, has been isolated also from an aged solution in crystalline form. The simplicity of the spectrum and relative signal intensities (tmeda; cytosine; 2,2′-bpy) strongly suggest that this complex is the symmetrical PtPdPt species with head−tail arranged 1-MeC$^-$ ligands (I5 in Figure 3).

Pd Coordination to 1: Where first? The X-ray crystal structures of compounds **2** and **3** tentatively suggest that it is the deprotonated amino groups of the 1-MeC ligands which bind to Pd first, followed by O2 in the case of complex **3**. Intuitively, one might have expected the contrary, hence that the lone electron pairs at the exocyclic O2 oxygen atom are the first sites ("anchors") of attack of Pd. On the other hand, it is clear that initial Pt coordination to N3 of 1-MeC reduces the (already low) basicity of O2 further, while increasing the acidity of the amino group $N4H_2$. While arguments concerning a preferential initial binding of Pd to N4 are strongly supported in the case of **2**, the situation with Pd2 in complex **3** is less straightforward in that it might reflect chelate ring-opening rather than formation. To make things even more complicated, it cannot be ruled out that the amine ligands at Pt have an influence on this matter. In summary, the question of two possible routes (Figure 3, left) to mixed $N4H^-$/O2 chelation of Pd starting from a head−tail structure of **1**, binding first to O2 or to N4, cannot be rigorously answered at present, although initial N4 coordination seems to be more consistent with our structural results.

Symmetrical Head−Tail PdPtPd Species. In a previous study, we had shown that *cis*-$[Pt(NH_3)_2(1\text{-MeC-}N3)_2]^{2+}$, when reacted with an excess of $[Pd(en)(H_2O)_2]^{2+}$, gives the trinuclear complex *cis*-$[Pt(NH_3)_2(1\text{-MeC}^-)_2\{Pd(en)\}_2]^{4+}$, in which the two 1-MeC$^-$ ligands adopt a head−tail arrangement.[11] As pointed out above, we believe that the analogous complex (I5 in Figure 3) also eventually forms with (tmeda)Pd^{II}.

When we reacted **1** with (2,2′-bpy)Pd^{II} in a 1:1-ratio, one product (blue star, Figure 7) forms, among two to three others.

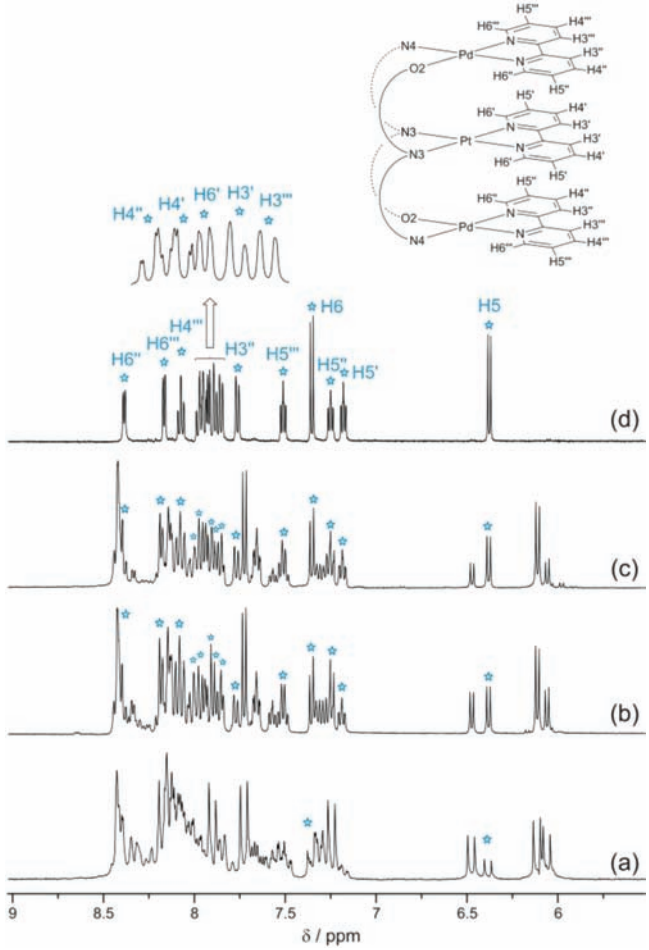

Figure 7. ^1H NMR spectra (D_2O, room temperature) of 1:1 mixtures of **1** with (2,2′-bpy)Pd^{II}: (a) after 12 h, pD 1.01; (b) after 2 days, pD 1.01; (c) after 2 days, pD adjusted to 5; (d) crystals of **4**, redissolved in D_2O (pD 7.03). Spectrum (a) was recorded at 200 MHz, spectra (b) and (c) were recorded at 400 MHz, and spectrum (d) was recorded at 500 MHz.

This product is the major one if an excess of (2,2′-bpy)Pd^{II} is applied. X-ray crystallography reveals this compound to be $[Pt(2,2'\text{-bpy})(1\text{-MeC}^-)_2\{Pd(2,2'\text{-bpy})\}_2](NO_3)_4\cdot 10.75H_2O$ (**4**). The cation has its 1-MeC$^-$ ligands oriented head−tail, hence in the very same way as in *cis*-$[Pt(NH_3)_2(1\text{-MeC}^-)_2\{Pd(en)\}_2]^{4+}$. Formation of **4** takes place at the astonishing low pD of ca. 1.[31] Given the relatively high pK_a values of the $N4H_2$ group of 1-MeC (ca. 16.7)[32] and of Pt-(1-MeC-*N*3) (estimated ca. 13)[33] and the moderate acidity of $[Pd(2,2'\text{-bpy})(H_2O)_2]^{2+}$ (pK_{a1} ≃ 4.80[34]), the ease of proton displacement from the amino group of the cytosine ligand is surprising indeed. A favorable orientation of the incoming (2,2′-bpy)Pd^{II} entity with

dx.doi.org/10.1021/ic3005097 | Inorg. Chem. 2012, 51, 6784−6793

respect to the exocyclic amino group of 1-MeC as a consequence of stacking between the two 2,2′-bpy rings might facilitate deprotonation of the $N4H_2$ group and Pd binding.

A comparison of the chemical shifts of the 1-MeC^- ligands in **4** with those of structurally analogous PdPtPd compounds with en and tmeda ligands at the two Pd atoms rather than 2,2′-bpy reveals marked differences (Table 1). In particular, the

Table 1. Chemical Shifts (δ, ppm, D_2O) of 1-MeC^- Resonances in Trinuclear Complexes *cis*-$[Pt(a)_2(1\text{-}MeC^-)_2\{Pd(a')_2\}_2]^{4+}$ with Head−Tail Arrangement of 1-MeC^-

a_2	$(a')_2$	H6	H5	CH_3
2,2′-bpy[a]	2,2′-bpy[a]	7.38	6.41	3.62
2,2′-bpy[b]	tmeda[b]	7.07	5.86	3.29
2,2′-bpy[b]	en[b]	7.06	5.85	3.32
$(NH_3)_2$[c]	en[c]	6.94	5.75	3.27

[a]Complex **4**. [b]Proposed assignment, compounds not isolated. [c]Ref 11.

significant downfield shift of 1-MeC^--H5 in **4** is to be noted. We attribute this primarily to an electron-withdrawing effect of the (2,2′-bpy)Pd^{II} entities bonded at N4. Figure 8 gives a view

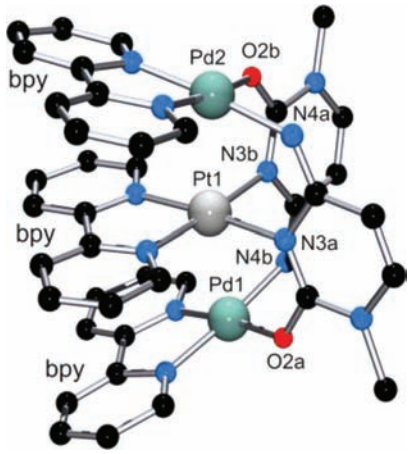

Figure 8. View of one of the two crystallographically different trinuclear cations **4**.

of one of the two crystallographically different trinuclear cations **4**. Both cations are almost identical, with head−tail orientation of the nucleobases and $\pi-\pi$ stacked (3.6 Å) bpy ligands.

This allows for relatively short Pt−Pd distances: Pt1−Pd1, 2.8091(10) Å; Pt1−Pd2, 2.8078(11) Å; Pt2−Pd3, 2.8040(10) Å; Pt2−Pd4, 2.7978(11) Å. Pd−Pt−Pd angles are 169.67(4)° and 169.53(4)° for Pt1 and Pt2, respectively. Metal coordination planes form dihedral angles of: $Pt1N_4/Pd1N_4$, 21.3(2)°; $Pt1N_4/Pd2N_4$, 21.2(2)°; $Pt2N_4/Pd3N_4$, 20.6(2)°; $Pt2N_4/Pd4N_4$, 20.8(2)°. The $\pi-\pi$-stacked bpy ligands display certain helicoidal rotation along the Pd−Pt−Pd vector, with torsion angle values ranging from 7.1(4)° (N11−Pt1−Pd2-N51) to 12.1(4)° (N11−Pt1−Pd1-N31). The N4−O2 distances, with N4 and O2 obviously not involved in mutual H bonding, between neighboring 1-methylcytosinate ligands are as follows: O2a−N4b, 2.851(14) Å; N4a−O2b, 2.882(15) Å; O2c−N4d, 2.885(15) Å; N4c−O2d, 2.78(2) Å. Platinum atoms (Pt1, Pt2) from both cations are nearly coplanar with the cytosine rings (distances from 0.03(2) to 0.13(2) Å), while Pd (Pd1, Pd2, Pd3, Pd4) atoms show longer distances to the cytosine planes, with O-bonded (0.74(2)−0.53(3) Å) metal ions again further away than N-bonded ones (0.054(3)−0.21(3) Å).

When cations of **4** are compared with the reported centrosymmetrical complex *cis*-$[Pt(NH_3)_2(1\text{-}MeC^-)_2\{Pd(en)\}_2]^{4+}$,[11] some geometrical differences should be addressed. First, the Pt−Pd distance is longer in the earlier reported case (2.9365(6) Å), and the intermetallic Pd−Pt−Pd angle is smaller (166.79(2)°). Second, the dihedral angles between coordination planes of Pt and Pd are considerably larger in the reported complex, namely, 32.4°. Third, torsion angles are 8.9° and 16.6° between ammine and en ligands and 32.1° between both en ligands. Fourth, the N4−O2 separation between 1-MeC^- ligands is 2.95 Å, significantly longer than in **4**. All these differences are probably a consequence of the bpy stacking present in **4**, which makes its structure somewhat more compact.

Pentanuclear Chain PdPtAgPtPd. Cocrystallization of the head−head dinuclear complex $[Pt(2,2'\text{-bpy})(1\text{-}MeC^-)_2Pd(en)]$ $(NO_3)_2\cdot 5H_2O$ (**2**) with $AgNO_3$ yielded a linear chain complex containing three different metal ions, namely, Pt, Pd, and Ag: $[\{Pt(2,2'\text{-bpy})(1\text{-}MeC^-)_2Pd(en)\}_2Ag](NO_3)_5\cdot 14H_2O$ (**5**). In Figure 9, the pentanuclear cation is shown. Ag^+ is

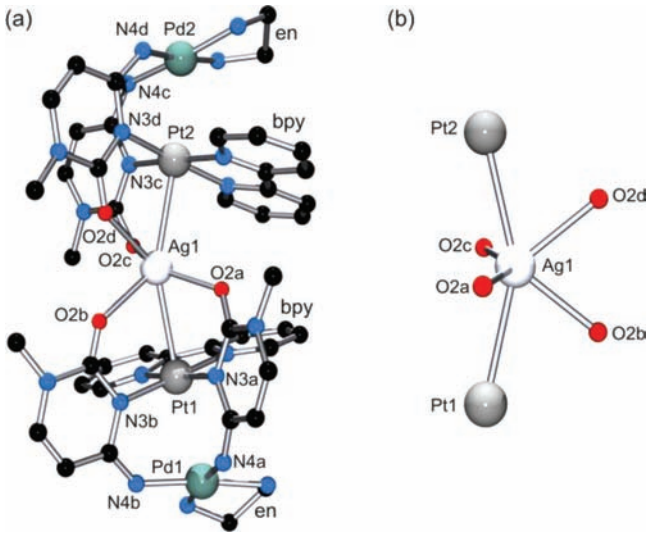

Figure 9. (a) View of pentanuclear cation **5**. (b) Detail of the coordination sphere of Ag^+ in complex **5**.

surrounded by four O2 oxygen atoms of 1-MeC^- ligands and adopts a distorted tetrahedral coordination geometry (Figure 9b). It displays two short and two long Ag−O bond distances: Ag1−O2a, 2.254(7) Å; Ag1−O2c, 2.274(7) Å; Ag1−O2b, 2.400(8) Å; Ag1−O2d, 2.433(8) Å. Besides, two of the O−Ag−O angles are considerably out of the range typically seen in tetrahedral coordination spheres: O2b−Ag1−O2d, 74.0(3)°, and O2a−Ag1−O2c, 141.8(3)°. The opening of the latter seems to allow for two additional weak metal−metal donor interactions (Pt1→Ag1 and Pt2→Ag1) in the coordination sphere of the silver atom. Ag^+ bridges both platinum atoms, forming a Pt1−Ag1−Pt2 angle of 153.76(4)°, with Ag−Pt distances of Ag1−Pt1, 3.0554(9) Å, and Ag1−Pt2, 3.0324(9) Å. The Pd−Pt−Ag angles are 170.40(3)° (Pd1−Pt1−Ag1) and 171.71(3)° (Pd2−Pt2−Ag1). The related coordination polymer, *cis*-$[\{Pt(NH_3)_2(1\text{-}MeC^-)\}_2Ag](NO_3)_3\cdot H_2O$,[7] which dis-

dx.doi.org/10.1021/ic3005097 | Inorg. Chem. 2012, 51, 6784−6793

plays strong Pt→Ag dative interactions and Ag^+ coordination to the exocyclic O2 groups of 1-MeC (of a ht-dimer, however), shows significantly shorter Ag−Pt distances (from 2.7972(11) Å to 2.9925(14) Å) and Ag−O bond lengths in the range of the long distances of the Ag1−O2b and Ag1−O2d bonds. In addition, a similar compound, consisting of a Pt_2AgPt_2 chain has previously been reported by our group, albeit with bridging 1-methyluracilato ligands.[35] Distances with the chain are 2.949(2) Å (Pt−Pt) and 2.787(1) Å (Pt−Ag), and interestingly, there exist relatively short intermolecular distances of 3.246(2) Å between platinum atoms of different cations.

Both monomeric units (Pt1−Pd1 and Pt2−Pd2) of complex **5** are analogous to cation **2**, with some structural differences. Along with their opposite arrangement with respect to the silver cation, they exhibit rotation of 85.8° (average) relative to each other. Dihedral angles between coordination planes of Pt^{II} and Pd^{II} are wider: $Pt1N_4/Pd1N_4$, 31.6(3)°, and $Pt2N_4/Pd2N_4$, 30.7(3)°. Following the tendency of these kind of complexes, distances from the N4-coordinated Pd^{II} atoms to the plane defined by 1-MeC rings are Pd1−1-$MeC_{(A)}$, 0.581(19) Å; Pd1−1-$MeC_{(B)}$, 0.484(19) Å; Pd2−1-$MeC_{(C)}$, 0.443(19) Å; Pd2−1-$MeC_{(D)}$, 0.432(19) Å.

Pt−Pd distances are 2.9476(9) Å (Pt1−Pd1) and 2.9430(10) Å (Pt2−Pd2). Both distances, as mentioned above, are in the range of analogous dimers with noninteracting (chelate) ligands. This situation agrees with the longer distances from the bpy planes to the en-CH_2 atoms exhibited in **5**: C3 (4.001(16) Å) and C2 (4.65(2) Å) in (en)Pd1 and C6 (3.951(17) Å) and C7 (4.723(16) Å) in (en)Pd2. Respective distances involving carbon atoms of the en group in complex **2** are considerably shorter: 3.737(11) and 4.471(11) Å. Concerning the packing, pentanuclear cations of **5** are surrounded by nitrate anions and numerous water molecules, building an intricate hydrogen bonding network. No direct interaction between cations of **5** is observed.

CONCLUSIONS

For the first time, a dinuclear PtPd complex (**2**) with two cis-arranged 1-methylcytosinato (1-MeC^-) ligands in head−head orientation has been crystallized and X-ray structurally characterized by reacting $[Pt(2,2'\text{-bpy})(1\text{-MeC})_2]^{2+}$ (**1**) with $(en)Pd^{II}$. A second representative displaying this coordination pattern, a pentanuclear PdPtAgPtPd complex (**5**), obtained by cocrystallizing **2** with $AgNO_3$, was likewise characterized. Despite its structural similarity with related dinuclear 1-methyluracilato (1-MeU^-) complexes, the packing and hydrogen bonding pattern of **2** is markedly different from corresponding 1-MeU^- species as a consequence of the differences in am(m)ine ligands at the Pt^{II} and the difference in the exocyclic 4-positions of the pyrimidine nucleobases. It is unclear at present why other Pd species such as $(tmeda)Pd^{II}$ and $(2,2'\text{-bpy})Pd^{II}$ do behave differently when reacted with **1** by forming trinuclear PdPtPd compounds with head−tail arranged 1-MeC^- ligands. At most for the PdPtPd compound **4** with its three 2,2′-bpy ligands, a kinetic reason, favorable stacking interactions combined with a higher acidity of the aqua ligands bonded to Pd, might be proposed to account for the preferential reaction of the head−tail rotamer of **1** with Pd^{II}.

ASSOCIATED CONTENT

Supporting Information

Additional spectroscopic NMR information and X-ray data of complexes reported. This material is available free of charge via the Internet at http://pubs.acs.org.

AUTHOR INFORMATION

Corresponding Author

*E-mail: bernhard.lippert@tu-dortmund.de Fax: (+49)231-755-3797 (B.L.); pablo.sanz@unizar.es (P.J.S.M.).

Notes

The authors declare no competing financial interest.

ACKNOWLEDGMENTS

This work was supported by the Deutsche Forschungsgemeinschaft, the Fonds der Chemischen Industrie, and the TU Dortmund. P.J.S.M. thanks the Spanish Ministerio de Economía y Competitividad for funding through the "Ramón y Cajal" program.

REFERENCES

(1) For early reviews, see (a) Weser, U. *Struct. Bonding (Berlin)* **1968**, *5*, 41. (b) Daune, M. *Met. Ions Biol. Syst.* **1974**, *3*, 1. (c) Hodgson, D. J. *Prog. Inorg. Chem.* **1977**, *23*, 211. (d) Marzilli, L. G. *Prog. Inorg. Chem.* **1977**, *23*, 255. (e) Barton, J. K.; Lippard, S. J. In *Nucleic Acid-Metal Ion Interactions*; Spiro, T. G., Ed.; John Wiley & Sons; New York, 1980; p 32.

(2) For more recent reports, see various articles in (a) Hud, N. V., Ed.; *Nucleic Acid-Metal Ion Interactions*; Royal Society of Chemistry Publishing: Cambridge, 2009. (b) Hadjiliadis, N., Sletten, E., Eds. *Metal Complex-DNA Interactions*; Wiley-VCH: Weinheim, 2009. (c) Sigel, A., Sigel, H., Sigel, R. K. O., Eds. *Interplay between Metal Ions and Nucleic Acids*; Springer: Dordrecht, 2012.

(3) See, e.g., (a) Cramer, R. E.; Dahlstrom, P. J. *J. Am. Chem. Soc.* **1979**, *101*, 3679. (b) Dijt, F. J.; Canters, G. W.; den Hartog, J. H. J.; Marcelis, A. J. M.; Reedijk, J. *J. Am. Chem. Soc.* **1984**, *106*, 3644. (c) Reily, M. D.; Marzilli, L. G. *J. Am. Chem. Soc.* **1986**, *108*, 6785. (d) Kozelka, J.; Fouchet, M. H.; Chottard, J. C. *Eur. J. Biochem.* **1992**, *205*, 894. (e) Holthenrich, D.; Sóvágó, I.; Fusch, G.; Erxleben, A.; Fusch, E. C.; Rombeck, I.; Lippert, B. *Z. Naturforsch.* **1995**, *50b*, 1767; (f) **1996**, *51b*, 1368.

(4) (a) Gariepy, K. C.; Curtin, M. A.; Clarke, M. J. *J. Am. Chem. Soc.* **1989**, *111*, 4947. (b) Roat, R. M.; Reedijk, J. *J. Inorg. Biochem.* **1993**, *52*, 263. (c) Choi, S.; Cooley, R. B.; Voutchkova, A.; Leung, C. H.; Vastag, L.; Knowles, D. E. *J. Am. Chem. Soc.* **2005**, *127*, 1773.

(5) (a) Šponer, J. E.; Sanz Miguel, P. J.; Rodríguez-Santiago, L.; Erxleben, A.; Krumm, M.; Sodupe, M.; Šponer, J.; Lippert, B. *Angew. Chem., Int. Ed.* **2004**, *43*, 5396. (b) Arpalahti, J.; Klika, K. D. *Eur. J. Inorg. Chem.* **2003**, 4195. (c) Klika, K. D.; Arpalahti, J. *Chem. Commun.* **2004**, 666.

(6) See, e.g., (a) Clarke, M. J. *J. Am. Chem. Soc.* **1978**, *100*, 5068. (b) Lippert, B.; Schöllhorn, H.; Thewalt, U. *J. Am. Chem. Soc.* **1986**, *108*, 6616. (c) Viljanen, J.; Klika, K. D.; Sillanpää, R.; Arpalahti, J. *Inorg. Chem.* **1999**, *38*, 4924. (d) Sanz Miguel, P. J.; Lax, P.; Willermann, M.; Lippert, B. *Inorg. Chim. Acta* **2004**, *357*, 84552. (e) Garijo Añorbe, M.; Welzel, T.; Lippert, B. *Inorg. Chem.* **2007**, *46*, 8222 and refs. cited.

(7) Yin, L.; Sanz Miguel, P. J.; Shen, W.-Z.; Lippert, B. *Chem.—Eur. J.* **2009**, *15*, 10723.

(8) (a) Matsumoto, K.; Sakai, K. *Adv. Inorg. Chem.* **2000**, *49*, 375. (b) Zangrando, E.; Pichierri, F.; Randaccio, L.; Lippert, B. *Coord. Chem. Rev.* **1996**, *156*, 275.

(9) See, e.g., (a) Verma, S.; Mishra, A. K.; Kumar, J. *Acc. Chem. Res.* **2010**, *43*, 79 and refs cited. (b) Chifotides, H. T.; Dunbar, K. R. *Acc. Chem. Res.* **2005**, *38*, 146. (c) Houlton, A. *Adv. Inorg. Chem.* **2002**, *53*, 87.

(10) For more recent publications, see, e.g., (a) Kampf, G.; Sanz Miguel, P. J.; Morell Cerdà, M.; Willermann, M.; Schneider, B.; Lippert, B. *Chem.—Eur. J.* **2008**, *14*, 6882. (b) Djinovic, V. M.; Galanski, M.; Arion, V. B.; Keppler, B. K. *Dalton Trans.* **2010**, *39*, 3633. (c) Ruiz, J.; Cutillas, N.; Vicente, C.; Villa, M. D.; López, G.; Lorenzo, J.; Avilés, F. X.; Moreno, V.; Baustita, D. *Inorg. Chem.* **2005**, *44*, 7365.
(11) Holthenrich, D.; Zangrando, E.; Chiarparin, E.; Lippert, B.; Randaccio, L. *J. Chem. Soc., Dalton Trans.* **1997**, 4407.
(12) See, e.g., (a) Micklitz, W.; Riede, J.; Huber, B.; Müller, G.; Lippert, B. *Inorg. Chem.* **1988**, *27*, 1979. (b) Micklitz, W.; Müller, G.; Huber, B.; Riede, J.; Rashwan, F.; Heinze, J.; Lippert, B. *J. Am. Chem. Soc.* **1988**, *110*, 7084. (c) Trötscher, G.; Micklitz, W.; Schöllhorn, H.; Thewalt, U.; Lippert, B. *Inorg. Chem.* **1990**, *29*, 2541 and refs. cited.
(13) See, e.g., (a) Oleksy, A; Blanco, A. G.; Boer, R.; Usón, I.; Aymamí, J.; Rodger, A.; Hannon, M. J. *Angew. Chem., Int. Ed.* **2006**, *45*, 1227 and refs cited. (b) Galindo, M. A.; Olea, D.; Romero, M. A.; Gómez, J.; Castillo, P.; del; Hannon, M. J.; Rodger, A.; Zamora, F.; Navarro, J. A. R. *Chem.—Eur. J.* **2007**, *13*, 5075 and refs. cited.
(14) As demonstrated by Marzilli et al., substituted 2,2′-bpy coligands of Pt^{II} are well suited to slow down the rotational dynamics in bis(nucleotide) complexes: Maheshwari, V.; Marzilli, P. A.; Marzilli, L. G. *Inorg. Chem.* **2008**, *47*, 9303.
(15) Kistenmacher, T. J.; Rossi, M.; Caradonna, J. P.; Marzilli, L. G. *Adv. Mol. Relax. Interact. Proc.* **1979**, *15*, 119.
(16) McCormick, B. J.; Jaynes, E. N., Jr.; Kaplan, R. I. *Inorg. Synth.* **1972**, *13*, 217.
(17) McCormick, B. J.; Jaynes, E. N., Jr.; Kaplan, R. I. *Inorg. Synth.* **1972**, *13*, 216.
(18) De Graaf, W.; Boersma, J.; Smeets, J. J. W.; Spek, A. L.; Van Kosten, G. *Organometallics* **1989**, *8*, 2907.
(19) Shen, W.-Z.; Trötscher-Kaus, G.; Lippert, B. *Dalton Trans.* **2009**, 8203.
(20) pH meter WTM Walheim "Ino-Lab pH Level 1".
(21) *CrysAlisPro*; Oxford Diffraction: Poland, 2008.
(22) (a) Sheldrick, G. M. *SHELX97*; University of Göttingen: Göttingen, Germany, 1998. (b) Farrugia, L. J. *J. Appl. Crystallogr.* **1999**, *32*, 837.
(23) The spectrum of **1** shown in ref 12 (Figure 3) contained, besides the two rotamer forms of **1**, also a minor impurity of free 1-MeC. In the present study, this impurity was absent (c.f. Supporting Information and also Figure 1a in next paragraph).
(24) (a) Faggiani, R.; Lippert, B.; Lock, C. J. L.; Speranzini, R. A. *J. Am. Chem. Soc.* **1981**, *103*, 111. (b) Sanz Miguel, P. J.; Roitzsch, M.; Yin, L.; Lax, P. M.; Holland, L.; Krizanovic, O.; Lutterbeck, M.; Schürmann, M.; Fusch, E. C.; Lippert, B. *Dalton Trans.* **2009**, 10774.
(25) Krumm, M.; Mutikainen, I.; Lippert, B. *Inorg. Chem.* **1991**, *30*, 884.
(26) See, e.g, (a) Micklitz, W.; Riede, J.; Huber, B.; Müller, G.; Lippert, B. *Inorg. Chem.* **1988**, *27*, 1979. (b) Micklitz, W.; Renn, O.; Schöllhorn, H.; Thewalt, U.; Lippert, B. *Inorg. Chem.* **1990**, *29*, 1836.
(27) Schöllhorn, H.; Thewalt, U.; Lippert, B. *Inorg. Chim. Acta* **1984**, *93*, 19.
(28) Neugebauer, D.; Lippert, B. *J. Am. Chem. Soc.* **1982**, *104*, 6596.
(29) (a) Krumm, M.; Lippert, B.; Randaccio, L.; Zangrando, E. *J. Am. Chem. Soc.* **1991**, *113*, 5129. (b) Krumm, M.; Zangrando, E.; Randaccio, L.; Menzer, S.; Lippert, B. *Inorg. Chem.* **1993**, *32*, 700. (c) Krumm, M.; Zangrando, E.; Randaccio, L.; Menzer, S.; Danzmann, A.; Holthenrich, D.; Lippert, B. *Inorg. Chem.* **1993**, *32*, 2183. (d) Mealli, C.; Pichierri, F.; Randaccio, L.; Zangrando, E.; Krumm, M.; Holthenrich, D.; Lippert, B. *Inorg. Chem.* **1995**, *35*, 3418.
(30) Mascharak, P. K.; Williams, I. D.; Lippard, S. J. *J. Am. Chem. Soc.* **1984**, *106*, 6428.
(31) The pD value of a typical ^{1}H NMR sample of $[Pd(2,2'\text{-bpy})(D_2O)_2]^{2+}$ is ca. 1.8 and drops to ca. 1 following deprotonation of $N4H_2$ and Pd^{II} coordination.
(32) Stewart, R.; Harris, M. G. *Can. J. Chem.* **1997**, *55*, 3807.
(33) Sanz Miguel, P. J.; Lax, P.; Lippert, B. *J. Inorg. Biochem.* **2006**, *100*, 980.
(34) Summa, N.; Schiessl, W.; Puchta, R.; van Eikema Hommes, N.; van Eldik, R. *Inorg. Chem.* **2006**, *45*, 2948.
(35) (a) Lippert, B.; Neugebauer, D. *Inorg. Chem.* **1982**, *21*, 451. (b) Lippert, B.; Schöllhorn, H.; Thewalt, U. *Inorg. Chem.* **1987**, *26*, 1736.